

Effects of angiotensin II on the pericyte-containing microvasculature of the rat retina

Hajime Kawamura¹, Masato Kobayashi¹, Qing Li¹, Shigeki Yamanishi¹, Kozo Katsumura¹, Masahiro Minami¹, David M. Wu^{1,2} and Donald G. Puro^{1,2,3}

¹Department of Ophthalmology & Visual Sciences, ²Neuroscience Graduate Program and ³Department of Molecular and Integrative Physiology, University of Michigan, Ann Arbor, MI 48105, USA

The aim of this study was to identify the mechanisms by which angiotensin II alters the physiology of the pericyte-containing microvasculature of the retina. Despite evidence that this vasoactive signal regulates capillary perfusion by inducing abluminal pericytes to contract and thereby microvascular lumens to constrict, little is known about the events linking angiotensin exposure with pericyte contraction. Here, using microvessels freshly isolated from the adult rat retina, we monitored pericyte currents via perforated-patch pipettes, measured pericyte calcium levels with fura-2 and visualized pericyte contractions and lumen constrictions by time-lapse photography. We found that angiotensin activates nonspecific cation (NSC) and calcium-activated chloride channels; the opening of these channels induces a depolarization that is sufficient to activate the voltage-dependent calcium channels (VDCCs) expressed in the retinal microvasculature. Associated with these changes in ion channel activity, intracellular calcium levels rise, pericytes contract and microvascular lumens narrow. Our experiments revealed that an influx of calcium through the NSC channels is an essential step linking the activation of AT₁ angiotensin receptors with pericyte contraction. Although not required in order for angiotensin to induce pericytes to contract, calcium entry via VDCCs serves to enhance the contractile response of these cells. In addition to activating nonspecific cation, calcium-activated chloride and voltage-dependent calcium channels, angiotensin II also causes the functional uncoupling of pericytes from their microvascular neighbours. This inhibition of gap junction-mediated intercellular communication suggests a previously unappreciated complexity in the spatiotemporal dynamics of the microvascular response to angiotensin II.

(Received 31 July 2004; accepted after revision 13 October 2004; first published online 14 October 2004)

Corresponding author D. G. Puro: Department of Ophthalmology and Visual Sciences, University of Michigan, 1000 Wall Street, Ann Arbor, MI 48105, USA. Email: dguro@umich.edu

The retina contains a rennin–angiotensin system (Kohler *et al.* 1997) that may play a role in regulating blood flow within this tissue. Consistent with this possibility, exposure to angiotensin II causes retinal arterioles, capillaries and venules to constrict, with smaller vessels being significantly more sensitive than the larger vessels (Schonfelder *et al.* 1998; Kulkarni *et al.* 1999). Thus, angiotensin II is likely to serve as a vasoactive signal regulating microvascular perfusion in the retina.

Candidates for regulating blood flow at the capillary level are the contractile pericytes, which are located on the abluminal wall of microvessels. By contracting or relaxing, these cells are thought to control capillary perfusion (Tilton, 1991; Schonfelder *et al.* 1998; Kawamura *et al.* 2003). Suggestive of the particular importance of these cells in the retinal microvasculature, the density of pericytes is higher in the retina than in other tissues

(Shepro & Morel, 1993). However, at present, there is only limited knowledge of the mechanisms by which vasoactive molecules, such as angiotensin II, regulate pericyte contractility and thereby lumen diameter and local blood flow. Consequently, the goal of this study was to identify events linking exposure of retinal microvessels to angiotensin II with pericyte contraction and vasoconstriction.

Based on the premise that ion channels are important in mediating functional responses to vasoactive signals, we assessed the effects of angiotensin II on the ionic currents in pericyte-containing microvessels. We now report that in microvessels freshly isolated from the rat retina, this eight-amino acid peptide activates several types of ion channels, including ones that provide pathways for extracellular calcium to enter pericytes. Our studies further revealed that an influx of calcium via nonspecific cation

channels is a key event linking the activation of angiotensin receptors with pericyte contraction and vasoconstriction. In addition, we found that angiotensin II reversibly inhibits cell-to-cell communication within retinal microvessels. As a result, this peptide not only regulates the contractility of individual pericytes, but also modifies the multicellular functional organization of the retinal microvasculature.

Methods

Microvessel isolation

Animal use conformed to the guidelines of the Association for Research in Vision and Ophthalmology and the University of Michigan Committee on the Use and Care of Animals. As detailed previously (Kawamura *et al.* 2003), 6- to 8-week Long-Evans rats (Harlan Sprague-Dawley, Inc., Indianapolis, IN and Charles Rivers, Cambridge, MA, USA) were killed with a rising concentration of carbon dioxide, and their retinas were rapidly removed and incubated in 2.5 ml Earle's balanced salt solution, which was supplemented with 0.5 mM EDTA, 20 mM glucose, 15 u papain (Worthington Biochemicals, Freehold, NJ, USA), and 2 mM cysteine for 30 min at 30°C and bubbled with 95% oxygen–5% carbon dioxide in order to maintain pH and oxygenation. After transfer to solution A (mm: 140 NaCl, 3 KCl, 1.8 CaCl₂, 0.8 MgCl₂, 10 Na-Hepes, 15 mannitol, and 5 glucose at pH 7.4 with osmolarity adjusted to 310 mosmol l⁻¹), each retina was then gently sandwiched between two glass coverslips (15 mm diameter, Warner Instrument Corp., Hamden, CT, USA). As reported previously (Sakagami *et al.* 1999a; Kawamura *et al.* 2003), vessels adhered to the coverslip that was in contact with the vitreal side of the retina. By repeating this tissue print step, several coverslips containing microvessels could be obtained from a retina. Figure 1 shows a photomicrograph of a segment of a freshly isolated pericyte-containing microvessel. Other photographs of retinal microvessels isolated by this method are in Sakagami *et al.* (1999), Oku *et al.* (2001) and Wu *et al.* (2001); in addition, a time-lapse video of an isolated

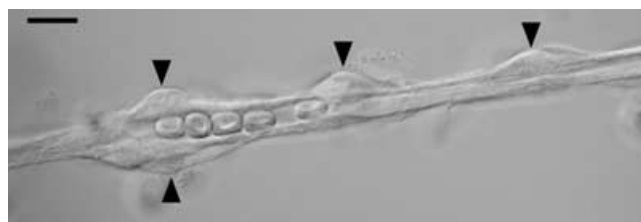


Figure 1. Differential interference contrast photomicrograph of a portion of a pericyte-containing microvessel freshly isolated from the rat retina

Arrowheads point to pericytes. Five red blood cells can be seen within the lumen. Scale bar = 10 μ m.

retinal microvessel is in the supplemental material. Our experiments were performed on microvessels that were >300 μ m in length.

Time-lapse photography

As detailed elsewhere (Kawamura *et al.* 2003; Wu *et al.* 2003), a glass coverslip containing isolated pericyte-containing microvessels was positioned in a perfusion chamber (volume = 200 μ l) on the stage of a Nikon Eclipse E800 equipped with differential interference contrast optics. Microvessels were viewed at $\times 1000$ magnification with the aid of a $\times 100$ oil objective. After a 2.67 min control period, microvessels were exposed for 5.33 min to an experimental solution and then re-exposed to the control perfusate (solution A). To facilitate detection of pericyte contractions, time-lapse images were recorded at 8 s intervals using a Nikon DCM1200 digital camera and ImagePro Plus software (Version 4.5, Media Cybernetics, Silver Spring MD, USA). The occasional pericytes (<5%) that spontaneously contracted and relaxed were not included in our analyses. As detailed previously (Wu *et al.* 2003), our calculation of the probability that responding pericytes were located near (≤ 30 μ m) capillary branch points was based on our observation that 20% of the length of the monitored microvessels was within 30 μ m of a bifurcation. Measurement of lumen diameters at sites adjacent to contracting pericytes was facilitated by use of ImagePro Plus software. Because contracting pericytes could cause microvascular lumens to move out of the narrow depth of focus available with differential interference contrast optics at high magnification, only those lumens that remained in focus throughout an experiment were included. During exposure to an experimental perfusate, lumen diameters were measured when the change in responsive vessels was maximal.

Calcium imaging

After freshly isolated microvessels were exposed to solution A supplemented with 1 μ M fura-2AM (Molecular Probes, Eugene, OR, USA) at 37°C for 30 min, the extracellular fura-2AM was washed out with solution A for at least 30 min. A coverslip containing microvessels with fura-loaded cells was positioned in a perfusion chamber (volume = 1 ml), which was perfused at ~ 2 ml min⁻¹. Digital imaging of fluorescence was performed at room temperature using an intensified CCD camera with a 12-bit dynamic range (Sensicam, Cooke Corp., Auburn Hills, MI, USA); the light source was a high-intensity mercury lamp coupled to a monochromator (Cairn Research Ltd, Faverhsam, UK). Imaging Workbench 5 (Indec BioSystems, Mountain View, CA, USA) was used to control the imaging equipment and collect data. Microvessels were viewed

at $\times 40$ using a Nikon Eclipse TE300 microscope equipped with a $\times 40$ oil-immersion objective. We measured fluorescent intensities at 340 nm and 380 nm from pericyte somas, which were defined as regions of interest (ROIs) using the imaging software. Subsequently, the 340:380 fluorescence ratio was calculated. Conversion to intracellular calcium concentration was achieved by using the equation of Grynkiewicz *et al.* (1985) in which R_{\min} and R_{\max} were determined by measuring the fluorescence ratio in fura-loaded pericytes located on freshly isolated microvessels exposed to calcium calibration buffer solutions (C-3009, Sigma) containing $0 \mu\text{M}$ and $39 \mu\text{M}$ free calcium and supplemented with the calcium ionophore, ionomycin ($5 \mu\text{M}$). Autofluorescence was not detected in the isolated retinal microvessels.

The basal concentration of pericyte calcium was defined as the mean concentration during the minute prior to angiotensin exposure. The peak increase in calcium level was defined as the mean of the three peri-peak determinations. The effect of nifedipine was assessed 1.5–3 min after the onset of exposure to the angiotensin-containing perfusate. We compared the mean calcium concentration during the 30 s period prior to nifedipine exposure with the maximal amount detected during exposure to this calcium channel blocker. In some experiments, we used a calcium-free perfusate that consisted of solution A without CaCl_2 and with 3 mM EGTA.

Electrophysiology

A coverslip containing microvessels was placed in a recording chamber, which was initially perfused with solution A. Vessels were examined at $\times 400$ magnification with an inverted microscope equipped with phase-contrast optics. Pericytes could be identified by their characteristic 'bump on a log' location on the abluminal wall of microvessels that had outer diameters of less than $7 \mu\text{m}$ (Kuwabara & Cogan, 1960; Sakagami *et al.* 1999). As detailed previously (Sakagami *et al.* 1999a), the perforated-patch configuration of the patch-clamp technique was used to monitor the ionic currents and the membrane potentials of pericytes located on microvessels that had been isolated from a retina within 3 h. The pipette solution consisted of (mM) 50 KCl, 64 K_2SO_4 , 6 MgCl_2 , 10 K-Hepes, $240 \mu\text{g ml}^{-1}$ amphotericin, and $240 \mu\text{g ml}^{-1}$ nystatin at pH 7.4 with the osmolarity adjusted to 280 mosmol l^{-1} . The pipettes, which had resistances of $\sim 5 \text{M}\Omega$, were mounted in the holder of a patch-clamp amplifier (Model 200B from Axon Instruments, Inc., Union City, CA or Model 3900 A from Dagan Corp., Minneapolis, MN, USA); seals of $\geq 10 \text{G}\Omega$ were made to the cell bodies of pericytes. As amphotericin/nystatin perforated the patch, the access

resistance to the pericytes studied decreased to less than $25 \text{M}\Omega$ within 5 min. As discussed previously (Sakagami *et al.* 1999; Li & Puro, 2001; Oku *et al.* 2001; Wu *et al.* 2001; Kawamura *et al.* 2002; Kawamura *et al.* 2003; Wu *et al.* 2003), it appears that the voltage could be clamped reasonably well for the identification of ionic conductances, despite the complex morphology of pericytes and the presence of gap junctions with other microvascular cells (Oku *et al.* 2001; Kawamura *et al.* 2002).

For continuous recordings of voltage, pericytes were clamped at zero current, and the voltage was sampled at 50 ms intervals. Adjustment for the calculated liquid junction potential (Barry, 1994) was made after data collection. In voltage-clamp experiments, the steady state current–voltage (I – V) relations were determined by recording the currents evoked by voltage-steps, which were controlled with pCLAMP 8 software (version 8.2, Axon Instruments), and were filtered at 1 kHz with a four-pole Bessel filter, digitally sampled at 1 ms intervals using a DigiData 1200B acquisition system (Axon Instruments) and stored by a computer equipped with pCLAMP and Origin (Version 7, OriginLab, Northampton, MA, USA) software for data analysis and graphics display. The mean current during the last 25 ms of each step was plotted *versus* the voltage of the step.

The amplitude of the nonspecific cation current was measured from recordings sampled at $500 \mu\text{s}$ intervals from pericytes voltage clamped at -103mV , which is the equilibrium potential for potassium. From these records, we also calculated the amplitude of the transient inward currents, which are generated by Cl_{Ca} channels (Sakagami *et al.* 1999); for each 1 s of sampling time, the transient inward current was calculated by subtracting the amplitude of the current that occurred in the absence of transient events from the average current amplitude, which was determined with pCLAMP software, as we have detailed previously (Kawamura *et al.* 2003). The amplitude of the peak Cl_{Ca} current was defined as the mean of the three peri-peak values.

In a series of experiments designed to determine the ionic selectivity of one of the angiotensin-induced conductances (summarized in Table 1 and Fig. 5), the recording pipettes were filled with (mM) 135 CsCl, 6 MgCl_2 and 10 Cs-Hepes at pH 7.4 and 280 mosmol l^{-1} ; microvessels were exposed to solution B (mM: 30 CsCl, 1.8 CaCl_2 , 1.8 BaCl_2 , 0.8 MgCl_2 , 10 Cs-Hepes, 5 glucose and 207 mannitol at pH 7.4) or modifications of solution B in which 43.6 mM choline chloride (the 'high chloride' group in Table 1 and Fig. 5), 30 mM NaCl ('high sodium'), 30 mM KCl ('high potassium') or 20 mM CaCl_2 ('high calcium') were added, and the concentration of mannitol was adjusted to maintain the osmolarity at 310 mosmol l^{-1} .

For analysis of the membrane capacitive currents, voltage-clamp recordings were filtered at 10 kHz and

Table 1. Effect of changes in the ionic composition of the bathing solution on the reversal potential (V_{rev}) of the angiotensin-induced current

| Extracellular solution | $[\text{Cl}^-]_o$ (mM) | $[\text{Na}^+]_o$ (mM) | $[\text{K}^+]_o$ (mM) | $[\text{Ca}^{2+}]_o$ (mM) | V_{rev} (mV) |
|------------------------|------------------------|------------------------|-----------------------|---------------------------|-----------------------|
| Solution B | 38.8 | 0 | 0 | 1.8 | -28 ± 2 |
| High chloride | 82.4 | 0 | 0 | 1.8 | -25 ± 4 |
| High sodium | 68.8 | 30 | 0 | 1.8 | $-7 \pm 2^*$ |
| High potassium | 68.8 | 0 | 30 | 1.8 | $-9 \pm 2^*$ |
| High calcium | 95.4 | 0 | 0 | 21.8 | $-8 \pm 2^*$ |

* $P < 0.001$. The composition of the extracellular solutions is detailed in the Methods section.

digitally sampled at 25 μs intervals; curve-fitting software (pCLAMP) was used to assess whether the decay of a membrane capacitive current fitted a first-order exponential function. Using pCLAMP software also facilitated our calculation of the area under the decaying capacitive current, i.e. the charge displacement, which was used as one indicator of the effect of angiotensin II on this current.

Chemicals

Unless otherwise noted, chemicals were obtained from Sigma.

Statistics

Data are given as means \pm s.e.m. Unless otherwise noted, probability was evaluated by the Student's t test, paired or unpaired, as appropriate.

Results

Angiotensin-induced vasoconstriction

We used time-lapse photography to monitor the effect of angiotensin II on pericyte-containing microvessels freshly isolated from the adult rat retina. In each of 36 monitored microvascular complexes, at least one pericyte contracted during exposure to 500 nM angiotensin II; induced relaxations were not observed. Of the 193 monitored pericytes that were exposed to 500 nM angiotensin II, reversible contractions were observed in 34%. Responding pericytes were observed at sites throughout the microvascular complexes; unlike muscarinic agonists (Wu *et al.* 2003), angiotensin II did not preferentially ($P = 0.3$, Fisher's exact test) induce contractions in pericytes positioned near vascular bifurcations.

The number of pericytes induced to contract was dependent upon the dose of angiotensin II (Fig. 2A), with the half-maximally effective concentration being ~ 15 nM. Consistent with the activation of AT_1 receptors mediating pericyte contraction, the selective agonist for

these receptors, L162313 (100 nM), effectively induced contractions within pericyte-containing microvessels (Fig. 2B). Associated with pericyte contraction, microvascular lumens narrowed (see the time-lapse movie in the supplemental material). During exposure to 500 nM angiotensin II, lumens adjacent to contracting pericytes narrowed by 54% ($P < 0.001$, Fig. 2C). From our time-lapse experiments, we concluded that freshly isolated microvessels provide a useful preparation in which to test hypotheses concerning the mechanism by which angiotensin II causes vasoconstriction in the retinal microvasculature.

Angiotensin-induced calcium increase

Because intracellular calcium regulates the contractility of pericytes (Kawamura *et al.* 2003; Wu *et al.* 2003), we hypothesized that this divalent cation plays a role in the response of these cells to angiotensin II. To begin to test this possibility, we incubated freshly isolated microvessels for 10 min in a bathing solution containing 10 μM BAPTA-AM (1,2-bis(2-aminophenoxy)ethane- N,N,N',N' -tetraacetic acid tetra(acetoxymethyl) ester), which is a cell-permeable calcium chelator. After this treatment, 500 nM angiotensin II failed to induce pericyte contractions (Fig. 2B); this was significantly ($P < 0.001$) different than the response rate in the absence of BAPTA. Our experiments using BAPTA support the idea that a change in intracellular calcium is an important step linking angiotensin exposure with pericyte contraction.

To help elucidate the mechanisms by which angiotensin II regulates the intracellular concentration of calcium, we monitored calcium levels in pericyte somas. As illustrated in Fig. 3 (left-hand panel), angiotensin II induced a transient increase in pericyte calcium when the perfusate lacked this divalent cation. In a series of experiments using a calcium-free perfusate (see Methods), the peak calcium increase during exposure to 500 nM angiotensin II was 123 ± 12 nM in the 44 of 52 monitored pericytes that had a detectable response. This increase was significantly ($P < 0.001$) above the basal

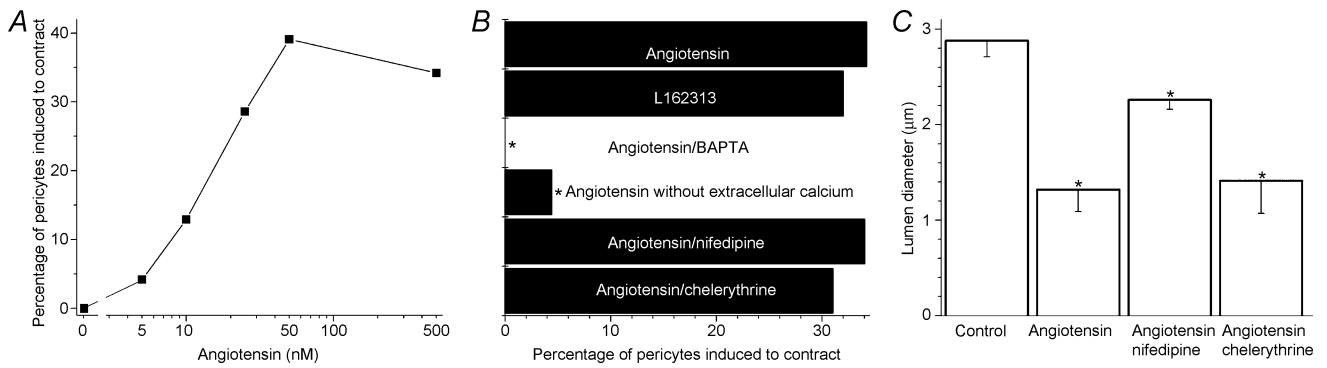


Figure 2. Effect of angiotensin II on the contractility of pericytes located on freshly isolated retinal microvessels

A, relationship between the concentration of angiotensin and the percentage of pericytes induced to contract. At angiotensin concentrations of ≥ 10 nM, the percentage of contracting pericytes was significantly ($P < 0.001$, Fisher's exact test) increased. The number of pericytes monitored by time-lapse photography was 292, 24, 31, 21, 23 and 193 for angiotensin concentrations of 0, 5, 10, 25, 50 and 500 nM, respectively. *B*, the contractile effect of angiotensin II and an AT₁ receptor agonist under various conditions. The labelled columns indicate the groups in which the perfusate (solution A) was supplemented with angiotensin II (500 nM), L162313 (100 nM), BAPTA-AM (10 μ M), nifedipine (10 μ M) or chelerythrine (1 μ M) or was modified by omitting CaCl₂ and adding 3 mM EGTA. Compared with the angiotensin group, $*P \leq 0.005$ (Fisher's exact test). The number of pericytes monitored by time-lapse photography was 193, 73, 41, 23, 73 and 68 for the angiotensin, L162313, BAPTA, calcium-free, nifedipine and chelerythrine groups, respectively. *C*, effect of 10 μ M nifedipine and 1 μ M chelerythrine on vasoconstriction induced by 500 nM angiotensin II. Compared with the control value, $*P \leq 0.005$ (Student's paired *t* test). The vasoconstriction induced by angiotensin in the presence of nifedipine was significantly ($P = 0.006$) less than the constriction induced in the absence of this calcium channel inhibitor. The presence of chelerythrine did not significantly ($P = 0.8$) affect the magnitude of the angiotensin-induced vasoconstriction. Because exposure to either nifedipine or chelerythrine did not significantly ($P > 0.1$) affect lumen diameter, the control value shown is the mean diameter of microvessels exposed to solution A without ($n = 12$) or with nifedipine ($n = 6$) or chelerythrine ($n = 6$). The number of monitored lumens was 24, 12, 6 and 6 for the control, angiotensin, angiotensin/nifedipine and angiotensin/chelerythrine groups, respectively. Error bars show s.e.m.

level. Because intracellular calcium levels rose despite the absence of calcium in the extracellular solution, we concluded that angiotensin II evokes a release of calcium from intracellular stores.

In contrast to the transient increase in pericyte calcium induced when angiotensin II was in a calcium-free perfusate, a plateau phase of increased calcium followed the peak increase when pericytes were exposed to

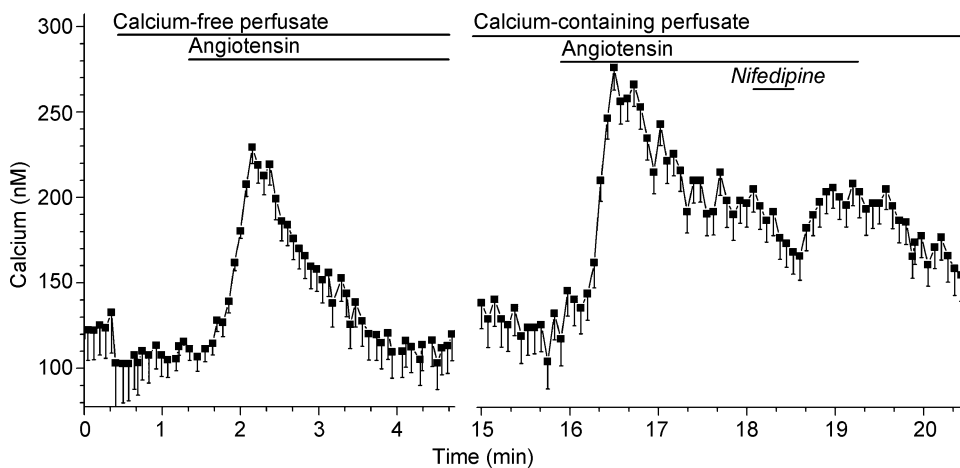


Figure 3. Angiotensin-induced changes in pericyte calcium

Plot of the mean intracellular calcium concentration *versus* time for 10 pericytes located on a freshly isolated microvascular complex; two other pericytes on this microvessel lacked detectable changes in their calcium levels. Left-hand panel, the perfusate was a modification of solution A in which CaCl₂ was omitted and 3 mM EGTA was added. Right-hand panel, the perfusate consisted of solution A, which contained 1.8 mM CaCl₂. Periods of exposure to 500 nM angiotensin II, 10 μ M nifedipine, the calcium-free perfusate and the calcium-containing perfusate (solution A) are shown by bars.

this peptide in a calcium-containing perfusate (Fig. 3, right-hand panel). During the plateau phase, the calcium concentration in the responding pericytes (50 of the 56 monitored cells) was 75 ± 3 nM greater than the basal calcium level; this was a significant ($P < 0.001$) increase. These experiments demonstrated that angiotensin II induces an influx of calcium, as well as its release from intracellular stores.

To determine whether the angiotensin-induced release of stored calcium was sufficient to trigger pericyte contraction, microvessels were monitored by time-lapse photography during exposure to 500 nM angiotensin II in a calcium-free perfusate. Under these conditions, a detectable contraction was induced in only 4% of the monitored pericytes (Fig. 2B). This was significantly ($P = 0.005$, Fisher's exact test) less than the 34% incidence of contracting pericytes observed during exposure of microvessels to 500 nM angiotensin II in the presence of extracellular calcium. Because the angiotensin-induced release of calcium rarely triggered pericyte contraction, it seems likely that an influx of extracellular calcium is a vital step linking angiotensin exposure with pericyte contraction.

Angiotensin-induced ionic conductances

To further elucidate the mechanisms by which angiotensin II affects the physiology of retinal capillaries,

we obtained patch-clamp recordings from pericytes located on freshly isolated microvessels. In the current-clamp recordings, the membrane potential of six of seven sampled pericytes decreased during exposure of microvessels to 500 nM angiotensin II. Specifically, the responding cells depolarized from -41 ± 2 mV to -26 ± 5 mV ($P < 0.014$). Subsequently, the membrane potential increased, but remained less than the resting level throughout a 5 min exposure to this peptide. The time course for the effect of angiotensin on the voltage of the responding pericytes is shown in Fig. 4A. With cessation of angiotensin exposure, repolarization occurred.

To establish the ionic basis for the angiotensin-induced depolarization, we recorded from voltage-clamped pericytes. As illustrated in Fig. 4B and C, comparison of the current-voltage relations before and 15–60 s after the onset of exposure of microvessels to 500 nM angiotensin II demonstrated that this peptide activated a depolarizing conductance, which was reversible. In a series of similar experiments ($n = 9$), we detected a depolarizing conductance in 89% of the sampled pericytes; the reversal potential of the angiotensin-induced current, i.e. the difference current between angiotensin and control, was -10 ± 2 mV (Fig. 4D). This induced inward current measured at -103 mV increased to a peak amplitude of 100 ± 8 pA at 18 ± 3 s ($n = 7$) after the onset of angiotensin exposure. In other voltage-clamp

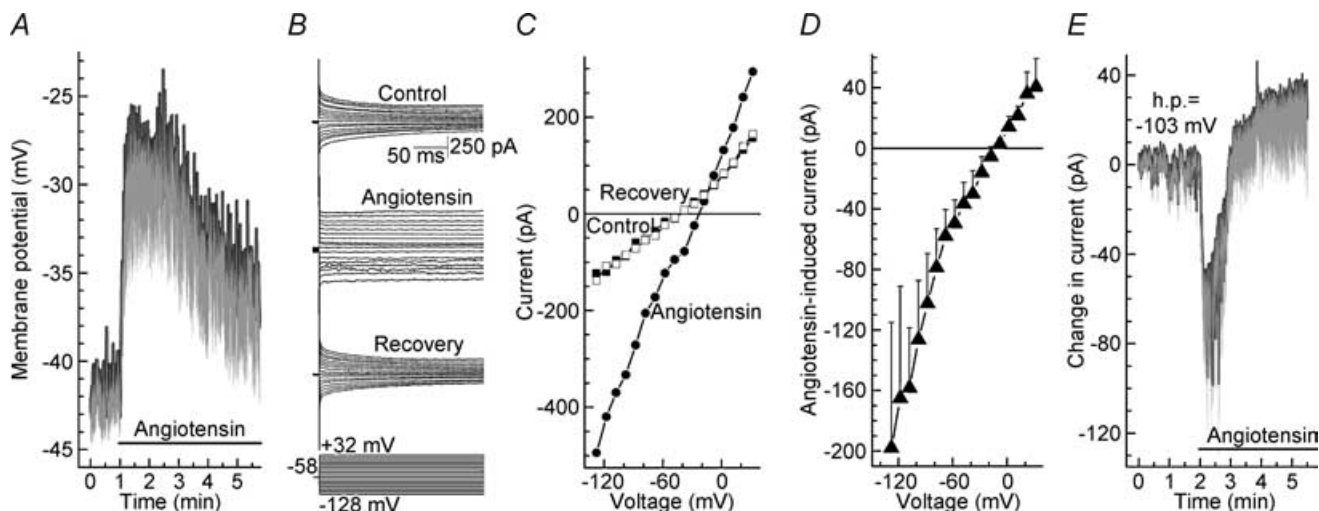


Figure 4. Effect angiotensin II on the electrophysiology of pericyte-containing retinal microvessels

A, time course for the effect of 500 nM angiotensin II (bar) on the membrane potential of pericytes ($n = 6$) located on freshly isolated microvessels. Voltage was sampled at 50 ms intervals; the black line shows the means and the vertical grey lines the s.e.m.s. B, current traces before angiotensin II exposure (Control), 15–60 s after the onset of exposure to 500 nM angiotensin II, and approximately 5 min after washout of angiotensin II. The clamp protocol is shown below. C, *I*-*V* plots of the steady-state currents shown in B. Control (■); Angiotensin II (●); Recovery (◇). D, mean angiotensin-induced current (difference between angiotensin and control) recorded in nine pericytes. E, time course for the effect of 500 nM angiotensin II (bar) on the current recorded in pericytes ($n = 7$) clamped at -58 mV and sampled at 50 ms intervals. To facilitate determination of the mean angiotensin-induced current, the current record was adjusted for each to the seven sampled pericytes so that at 2 min prior to exposure to angiotensin II, the current amplitude was 0 pA. The black line shows the means and the vertical grey lines the s.e.m.s of the adjusted current records.

experiments, we systematically varied the composition of the bathing solution in order to determine the ionic selectivity of this angiotensin-induced conductance. We observed that the reversal potential of this induced current was significantly ($P < 0.001$) affected by changes in the extracellular concentration of sodium, potassium and calcium, but was not significantly ($P = 0.54$) affected by changes in chloride (Fig. 5 and Table 1). From these findings, we concluded that this depolarizing conductance is generated by the activation of nonspecific cation (NSC) channels whose permeability ratio, based on the extended constant-field voltage equation with assumptions similar to those of Mayer and Westbrook (Mayer & Westbrook, 1987), is $P_{Ca}/P_{Na,K} = 3$. Thus, the angiotensin-activated NSC channels not only cause pericytes to depolarize, but also provide pathways for the entry of calcium ions.

In addition to activating an NSC conductance, angiotensin II also activated transiently occurring inward currents (Fig. 6A), which we previously demonstrated are generated by calcium-activated chloride (Cl_{Ca}) channels (Sakagami *et al.* 1999). For the seven of eight sampled pericytes that had conductances activated by 500 nM angiotensin II, the transient inward currents measured at -103 mV increased significantly ($P < 0.001$), from a basal level of 9.4 ± 4.3 pA to a peak of 42 ± 6 pA. The time course for the activation of the Cl_{Ca} conductance is shown in Fig. 6B. Consistent with these channels being activated by calcium, incubation of microvessels for 10 min in $10 \mu\text{M}$ BAPTA-AM prevented 500 nM angiotensin II from significantly ($P = 0.5$, $n = 6$) increasing the Cl_{Ca} conductance. In contrast, treatment with BAPTA-AM did not prevent angiotensin II from activating an NSC conductance whose peak amplitude was not significantly ($P = 0.3$, $n = 6$) different than when it was induced in the absence of BAPTA. Taken together, our electrophysiological experiments demonstrated that angiotensin II activates NSC and Cl_{Ca} channels; both of which cause pericytes to depolarize.

Role of calcium influx via voltage-dependent calcium channels

Because the angiotensin-induced depolarization is sufficient to activate the voltage-dependent calcium channels (VDCCs) expressed in the retinal microvasculature (Sakagami *et al.* 1999), we considered the possibility that these channels are important calcium influx pathways. To begin to assess the role of VDCCs in mediating the response to angiotensin II, we exposed microvessels to nifedipine, which we previously demonstrated blocks the L-type VDCC expressed by retinal pericytes (Sakagami *et al.* 1999, 2001). As illustrated in Fig. 3 (right-hand panel), the plateau phase of the angiotensin-induced increase in

pericyte calcium was partially diminished when the perfusate was supplemented with $10 \mu\text{M}$ nifedipine. On average, nifedipine diminished this angiotensin-induced increase by $35 \pm 4\%$ ($P < 0.001$, paired student's *t* test; $n = 12$ microvessels with 5 ± 2 pericytes monitored per complex).

Because opened VDCCs, as well as the angiotensin-activated NSC channels, would provide pathways for calcium influx, the question arose as to the role of these calcium channels in mediating the contractile response of pericytes during angiotensin exposure.

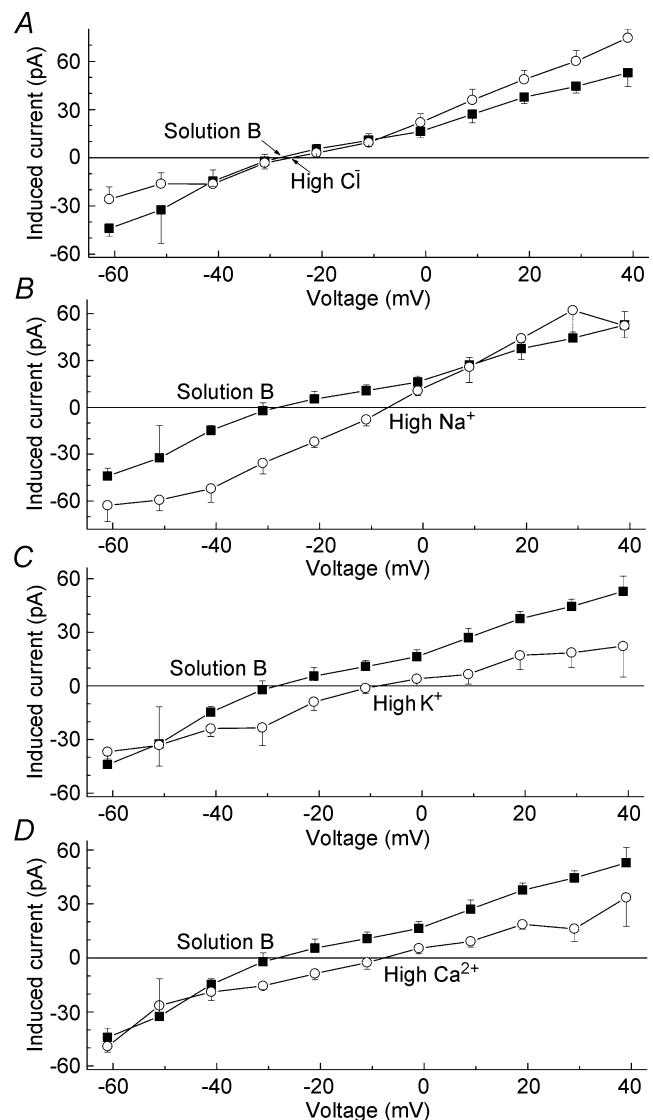


Figure 5. Effect of extracellular ions on the current-voltage relations of the angiotensin-induced current

The composition of the extracellular solutions is detailed in the Methods section. Data points show the mean with the s.e.m. of the steady-state currents induced by 500 nM angiotensin II. The number of sampled pericytes was 4, 3, 4, 7 and 5 for the solution B, high chloride, high sodium, high potassium and high calcium groups, respectively. Error bars show s.e.m.

Using time-lapse photography, we observed that 10 μM nifedipine did not significantly ($P = 1.0$, Fisher's exact test) affect the percentage of pericytes that were induced to contract during exposure 500 nM angiotensin II (Fig. 2B). On the other hand, this VDCC blocker did diminish the magnitude of the angiotensin-induced vasoconstriction (Fig. 2C). Specifically, in the presence of 10 μM nifedipine, 500 nM angiotensin II caused microvascular lumens at sites adjacent to contracting pericytes to narrow by $22 \pm 3\%$ ($n = 6$). Although this was a significant ($P = 0.001$) vasoconstriction, it was significantly ($P = 0.006$) less than the $54 \pm 8\%$ decrease in lumen diameter induced by 500 nM angiotensin II in the absence of this VDCC blocker. Thus, although VDCCs are not essential for the triggering of angiotensin-induced contractions, their activation enhances the contractile response and thereby the magnitude of the vasoconstriction.

Inhibition of cell-to-cell coupling

In addition to demonstrating that angiotensin II activates depolarizing NSC and Cl_{Ca} currents, our electrophysiological recordings also revealed that this peptide affects the membrane capacitive current. This is illustrated in Fig. 7A and also the current traces in Fig. 4B. This capacitive current is of interest because, as predicted from a modelling analysis (Lindau & Neher, 1988) and confirmed in our studies of pericytes located on retinal microvessels (Oku *et al.* 2001; Kawamura *et al.* 2003), the time course for the decay of the membrane capacitive current is fitted by a first-order exponential function when a cell is uncoupled, but is complex when a cell is electrotonically coupled to its neighbours. As reported previously (Oku *et al.* 2001; Kawamura *et al.* 2002; Kawamura *et al.* 2003), we observed that under control conditions, the membrane capacitive current recorded in pericytes has a complex rate of decay (Fig. 7A, left-hand

panel). However, approximately 20–60 s after the onset of exposure to 500 nM angiotensin II, the decay rate of the membrane capacitive current decreased in 16 of 21 monitored pericytes; subsequently the decay rate could be fitted by a first-order exponential function (Fig. 7A, right-hand panel). In agreement with hundreds of perforated-patch recordings done in our previous studies of pericyte-containing retinal microvessels, we did not observe in this study spontaneous changes in the capacitance transient during control periods ($n = 53$). The effect of angiotensin II on the membrane capacitive current was transient, as illustrated in Fig. 7B. After approximately 3 min of continued exposure to 500 nM angiotensin II, the decay rate of the membrane capacitive current again became complex. From this series of experiments, we concluded that angiotensin exposure results in the transient closure of the intercellular pathways that are known to electronically couple pericytes with their microvascular neighbours (Kawamura *et al.* 2003).

From earlier studies, we concluded that protein kinase C (PKC) regulates the gap junction pathways of retinal microvessels (Oku *et al.* 2001; Kawamura *et al.* 2002). For example, exposure to the PKC activator phorbol myristate markedly reduces gap junction-mediated intercellular communication (Oku *et al.* 2001). Based on the PKC-sensitivity of microvascular gap junctions, we considered the hypothesis that this enzyme plays a role in the angiotensin-induced uncoupling of pericytes. To test this idea, we exposed freshly isolated microvessels to chelerythrine (1 μM), which is a potent inhibitor of most PKC isoforms (Herbert *et al.* 1990), and prevented 500 nM angiotensin II from having a detectable effect on the membrane capacitive current recorded in each of seven sampled pericytes. This lack of effect in the presence of chelerythrine contrasted significantly ($P = 0.001$, Fisher's exact test) with our observation that in the absence of this PKC inhibitor, exposure to 500 nM angiotensin II switched the decay

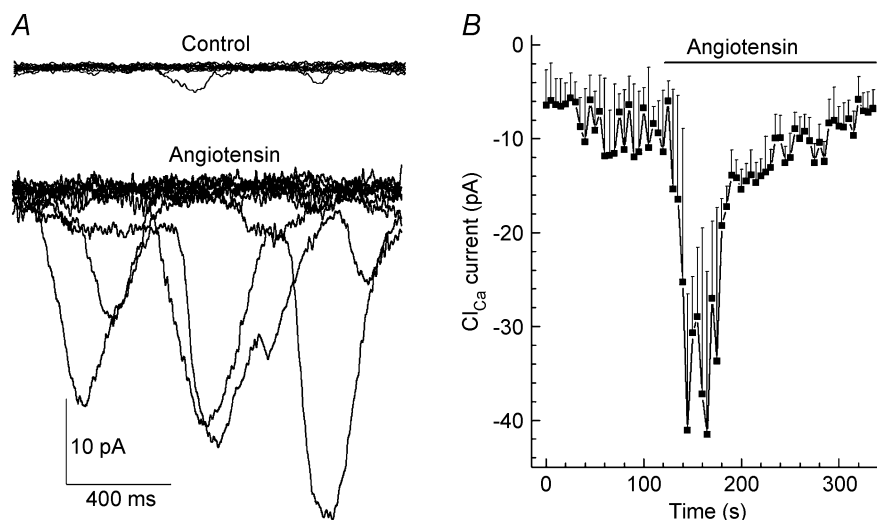


Figure 6. Effect of angiotensin II on calcium-activated chloride currents A, in each panel, 15 current traces of a pericyte held at -103 mV are superimposed to show transient inward currents before (Control) and 15–60 s after the onset of exposure to 500 nM angiotensin II. B, mean Cl_{Ca} current calculated at 5 s intervals before and during exposure to 500 nM angiotensin II (bar).

rate of the membrane capacitive current in 76% of the sampled pericytes ($n = 21$) from being complex to being fitted by a first-order exponential function.

In another series of experiments, we tested the hypothesis that the angiotensin-induced rise in calcium, which can activate a number of PKC isoforms, plays a role in the closure of the gap junctions that couple pericytes with their microvascular neighbours. Consistent with possibility, incubation of isolated microvessels for 36 ± 6 min in solution A supplemented with $10 \mu\text{M}$ BAPTA-AM prevented 500 nM angiotensin II from affecting the membrane capacitive current in each of four sampled pericytes. This contrasted significantly ($P = 0.004$, Fisher's exact test) with our observation that in the absence of this calcium chelator, 16 of 19 pericytes showed a change in the decay rate of the membrane capacitive current during exposure to 500 nM angiotensin II. Taken together, our experiments indicate that the rise in intracellular calcium and the activation of PKC are important steps leading to the inhibition of intercellular electrotonic transmission during exposure of retinal microvessels to angiotensin II.

Effect of chelerythrine on induced conductances and vasoconstriction

Having found that PKC is likely to play a role in the angiotensin-induced uncoupling of pericytes, we asked whether this enzyme was also critical for the angiotensin-induced activation of NSC and Cl_{Ca} conductances. However, inconsistent with this possibility, we found that chelerythrine did not prevent angiotensin from activating these currents in pericytes (Fig. 8A). Further, the peak amplitudes of the angiotensin-induced NSC and Cl_{Ca} currents were not significantly ($P > 0.07$) affected by this PKC inhibitor (Fig. 8B). Specifically, in the presence of $1 \mu\text{M}$ chelerythrine, 500 nM angiotensin II induced peak NSC and Cl_{Ca} currents (measured at -103 mV) of $118 \pm 26 \text{ pA}$ and $50 \pm 6 \text{ pA}$ ($n = 7$), respectively; in the absence of chelerythrine, the NSC and Cl_{Ca} amplitudes were $100 \pm 8 \text{ pA}$ and $33 \pm 6 \text{ pA}$, respectively. Also, the times-to-peak for these angiotensin-induced conductances were not significantly ($P \geq 0.18$) affected by chelerythrine. Thus, these experiments support the scenario that angiotensin II activates NSC and Cl_{Ca} channels by a PKC-independent mechanism.

In other experiments, we assessed the effect of chelerythrine ($1 \mu\text{M}$) on the angiotensin-induced contraction of pericytes. As with the induced NSC and Cl_{Ca} conductances, the percentage of pericytes contracting in response to 500 nM angiotensin II was not significantly ($P = 0.36$, Fisher's exact test) affected by this PKC inhibitor (Fig. 2B). We also observed that chelerythrine did not significantly ($P = 0.8$) affect the magnitude of the

angiotensin-induced vasoconstriction (Fig. 2C). From these experiments, we concluded that PKC activation is not an essential step in mediating pericyte contraction and vasoconstriction during exposure of retinal microvessels to angiotensin II. However, it appears that PKC does mediate the angiotensin-induced uncoupling of pericytes from their microvascular neighbours.

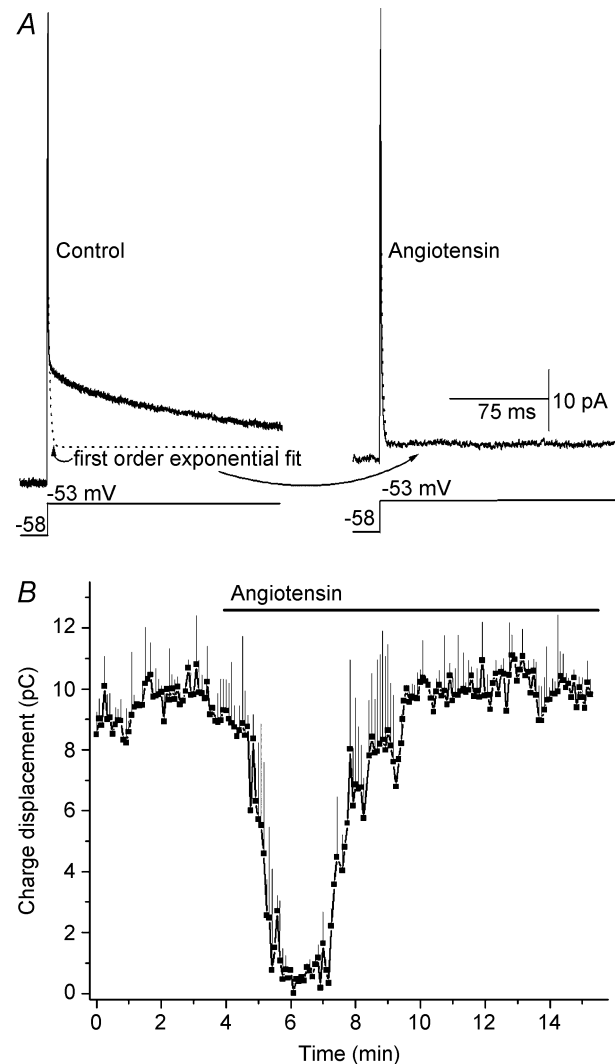


Figure 7. Effect of angiotensin II on the membrane capacitive current of pericytes located on a freshly isolated microvessels. **A**, left-hand panel, average of 10 traces (solid line) evoked by a voltage step from -58 to -53 mV under control conditions. The calculated first-order exponential fit is shown by the dotted line. Right-hand panel, for the same cell, the average current trace ($n = 10$) and the closely matched first-order exponential fit (dotted line) 2 min after the onset of exposure to 500 nM angiotensin II. **B**, time course for the effect of angiotensin on the capacitance transient. The area under the current trace evoked by a 200 ms voltage step from -58 to -38 mV was calculated at 2 s intervals before and during exposure of pericytes ($n = 4$) to 500 nM angiotensin II; this area, expressed in pA s^{-1} , i.e. pCoulombs , is a measure of the charge displacement during the capacitance transient.

Discussion

This study shows that angiotensin II alters the physiology of pericyte-containing retinal microvessels. Responses to this peptide include the activation of NSC and Cl_{Ca} conductances whose depolarizing effect on pericytes is sufficient to open VDCCs. In addition to changes in ion channel activity, we found that angiotensin II causes intracellular calcium levels to rise, pericytes to contract and microvascular lumens to narrow. Our experiments indicate that the influx of calcium through NSC channels is a critical step linking the activation of AT_1 angiotensin receptors with pericyte contraction and thereby vasoconstriction. Although not essential for triggering contraction, calcium entry via the VDCCs enhances the vasoconstrictive response of pericytes to angiotensin II. Unexpectedly, we found that angiotensin II not only regulates the contractility of pericytes, but also functionally uncouples these cells from their microvascular neighbours. Taken together, our observations support the hypothesis that angiotensin II serves as a vasoactive signal in the pericyte-containing retinal microvasculature and suggest a previously unappreciated complexity in the temporal and spatial dynamics of the microvascular response to this peptide.

This is the first report of angiotensin II regulating intercellular communication within blood vessels. Recently, we demonstrated the other vasoactive signals, i.e. endothelin-1 and ATP, also reversibly inhibit gap junction pathways within the retinal microvasculature (Kawamura *et al.* 2002, 2003). In our perforated-patch clamp studies of hundreds of pericytes located on freshly isolated retinal microvessels, a similar change in cell-to-cell

communication has never occurred spontaneously. Thus, we conclude that the inhibition of gap junction-mediated communication is a newly discovered mechanism by which certain signalling molecules regulate microvascular function.

The experiments reported in this study support the hypothesis that the closure of microvascular gap junctions during exposure to angiotensin II is mediated via a PKC-dependent mechanism. This is consistent with our earlier work demonstrating that the PKC activator, phorbol myristate, markedly reduces intercellular communication in retinal microvessels (Oku *et al.* 2001). However, because chelerythrine inhibits most isoforms of PKC (Herbert *et al.* 1990), it remains to be established which of the various PKC isoforms, i.e. α , β_2 , δ and ζ (Moriarty *et al.* 2000; Suzuma *et al.* 2002), that are expressed by retinal pericytes and endothelial cells play a role in the angiotensin-induced inhibition of cell-to-cell communication. However, our finding that a rise in pericyte calcium is required in order for angiotensin II to uncouple pericytes suggests a role for the calcium-dependent α , β_2 and/or δ isoforms. It is most likely that the activation by angiotensin of a PKC isoform inhibits the function of microvascular gap junctions by catalysing the phosphorylation of one or more the connexins, i.e. 43, 37 and 40, expressed in the pericyte-containing microvasculature of the retina (Li *et al.* 2003; Fernandes *et al.* 2004). Consistent with this idea, there is good evidence that the phosphorylation of connexins in a variety of cell types results in a reduction in the abundance of these molecules in the plasma membrane (Lampe *et al.* 2000). However, we posit that the rapid reversibility of the angiotensin-induced uncoupling

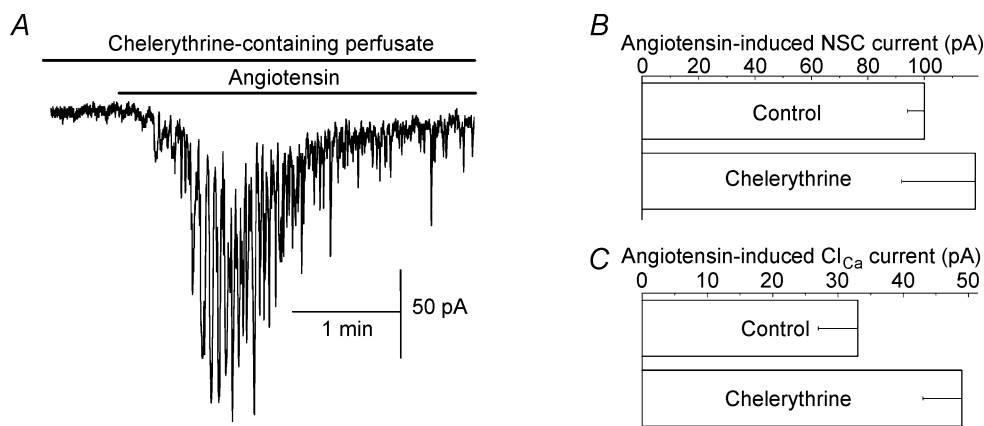


Figure 8. Effect of angiotensin II on pericyte currents during exposure of microvessels to chelerythrine. A, continuous current trace of a pericyte held at -103 mV and exposed to solution A supplemented with $1 \mu\text{M}$ chelerythrine and, during the period indicated by the bar, 500 nM angiotensin II. Superimposed on the relatively slowly changing NSC current are the transient Cl_{Ca} currents. Prior to this recording, the microvessel was maintained in the chelerythrine-containing solution for 30 min. B, C, peak amplitudes of the NSC and Cl_{Ca} currents induced by 500 nM angiotensin II in the absence and presence of $1 \mu\text{M}$ chelerythrine. For each group, seven pericytes were sampled; currents were measured at -103 mV. Neither induced conductance was significantly ($P > 0.36$) affected by chelerythrine.

of pericytes is probably explained by a transient functional inhibition of connexins that remain within the membrane of pericytes and endothelial cells. In agreement with this possibility, the phosphorylation of certain connexins is known to decrease their unitary conductance (Moreno *et al.* 1994). Goals for the future are to identify the specific type(s) of microvascular connexins and PKC isoforms that are regulated by angiotensin II in the retinal microvasculature.

Almost certainly the angiotensin-induced inhibition of electrotonic transmission profoundly influences the spatiotemporal characteristics of the microvascular response to this peptide. It seems likely that exposure to angiotensin II at a focal site along a microvessel would evoke widespread depolarization as the voltage change induced locally by the opening of NSC and Cl_{Ca} channels spreads electrotonically from cell to cell via gap junction pathways, which are known to extensively interconnect cells of the retinal microvasculature (Oku *et al.* 2001). However, this intercellular transmission would cease when angiotensin induces gap junction closure. As a result, vasoconstriction would then be restricted to the site directly exposed to this vasoactive peptide. Thus, this model for the actions of angiotensin II in the retinal microvasculature predicts that focally released angiotensin II would initially affect blood flow throughout a relatively large area of a microvascular network, but subsequently the decrease in perfusion would be delimited to the capillary segment directly exposed to this peptide. Perhaps, by transiently regulating perfusion in upstream vessels, angiotensin II quickly and effectively decreases local capillary perfusion without causing sustained and potentially harmful hypoperfusion in widespread areas of the retina. Clearly, future experimental studies are needed to fully characterize the spatiotemporal features of angiotensin's effects on retinal microvessels.

A finding of this and other recent studies of retinal microvessels (Kawamura *et al.* 2003; Wu *et al.* 2003) is that pericytes appear to be functionally heterogeneous with regard to their contractility. For example, in this study, maximal concentrations of angiotensin II evoked a contractile response in only ~40% of the pericytes. Even though limitations in the sensitivity of our contraction assay may underestimate the number of responding pericytes, it seems clear that there are significant qualitative differences in the contractile responses of these cells, although we cannot exclude that our procedure to isolate microvessels from the retina causes some pericytes to become noncontractile. The failure of a majority of the pericytes to contract does not appear to be due to their lacking an induced increase in intracellular calcium; angiotensin II caused the concentration of this divalent cation to increase in nearly all (~90%) monitored pericytes. Perhaps, the threshold at which a rising intracellular calcium concentration causes contraction

varies among the population of retinal pericytes. At present, the functional significance of retinal microvessels having a large population of pericytes that do not contract in response to a vasoactive signal remains to be established. However, since not all pericytes along a microvascular segment need to contract in order to reduce blood flow, the heterogeneity of pericyte contractility may provide an adaptive advantage by being energy efficient. With voltage changes being easily transmitted via gap junctions from noncontractile pericytes to those that do contract (Kawamura *et al.* 2003), retinal microvessels appear to be designed to maximize detection of localized extracellular signals while minimizing the energy needed to carry out the vasoactive response.

Our identification of the mechanisms by which angiotensin II regulates the contractility of retinal pericytes raised the question as to whether similar events take place in pericyte-containing microvessels located in nonretinal tissues. At present, the descending vasa recta of the kidney is the only other microvasculature in which angiotensin's effects on the membrane potential of pericytes, the calcium level in these cells and the diameter of vascular lumens are known (Pallone & Huang, 2002; Rhinehart *et al.* 2002; Zhang *et al.* 2002). Similar to the responses of retinal pericytes, exposure to angiotensin II causes vasa recta pericytes to depolarize, calcium levels to rise and microvascular lumens to narrow. An additional similarity of retinal and vasa recta microvessels (Zhang *et al.* 2002) is that VDCC inhibition diminishes, but does not abolish, the vasoconstriction induced by angiotensin II. This persistence of angiotensin-induced contraction despite VDCC inhibition indicates that an event, other than activation of these calcium channels, mediates the angiotensin-induced contraction of pericytes in both of these microvasculatures. In retinal microvessels, our experiments revealed that the opening of calcium-permeable NSC channels is likely to be an essential event linking the activation of angiotensin receptors with the triggering of pericyte contraction and lumen narrowing. Whether angiotensin-activated NSC channels also play a role in the response of pericyte-containing microvessels in nonretinal tissues remains to be determined. In fact, it may be that angiotensin's vasoactive effects on pericytes are transduced by different mechanisms in different vascular beds, as is the case for the effect of this peptide on vascular smooth muscle (Nagahama *et al.* 2000). Consistent with different pericyte-containing microvasculatures having different transduction mechanisms, PKC inhibition prevents angiotensin-induced vasoconstriction in the pericyte-containing vasa recta (Zhang *et al.* 2004), but not in the retinal microvasculature (Fig. 2C). Other differences in the action of this peptide may exist, but comparative data are limited. For example, it is not known whether angiotensin II causes a functional uncoupling

of vasa recta pericytes from other microvascular cells, as it does in the retinal microvessels. Also, it is not known whether reactive oxygen species mediate angiotensin's vasoconstrictive effect in microvessels of the retina, as they do in the descending vasa recta (Zhang *et al.* 2004). Nor do we know whether the pericyte contraction triggered by the activation of AT₁ receptors is modulated by the concomitant activation of AT₂ receptors, as occurs in vasa recta pericytes (Zhang *et al.* 2004). We speculate that the mechanisms mediating angiotensin's effects on a tissue's microvasculature have been selected to meet the specialized functional demands of that tissue. A challenge for the future is to determine the adaptive advantages of the various pathways by which angiotensin II can regulate the physiology of pericyte-containing microvessels.

Our conclusions concerning the mechanisms by which angiotensin II induces vasoconstriction in pericyte-containing microvessels are based on experiments using freshly isolated retinal microvessels. One benefit of studying microvessels in isolation is that confounding effects mediated by nonvascular retinal cells are eliminated. Also, it is possible to precisely control the concentrations of agonists and inhibitors, as well as the duration of exposure to these chemicals. Furthermore, in contrast to cultured pericytes, use of isolated microvessels permits electrophysiological, calcium-imaging and time-lapse studies to be performed while these cells are integral components of the microvasculature. This latter advantage is of particular importance because pericytes function as elements of multicellular functional units in which intercellular communication is mediated via gap junction pathways, which are regulated by vasoactive signals (Kawamura *et al.* 2002; Kawamura *et al.* 2003) and can be disrupted by pathophysiological conditions, such as diabetes (Oku *et al.* 2001). However, even though there are many experimental advantages to studying freshly isolated microvessels, caution must be exercised. For example, it remains to be demonstrated that the effects of angiotensin II on ion channels, calcium levels, pericyte contractility and cell-to-cell coupling occur *in vivo*. Hence, an *in vivo* application of the imaging and electrophysiological techniques used in this study would be ideal, although at present this does not appear to be feasible. Also, because intraluminal pressure is likely to affect microvascular physiology, development of methods to internally perfuse isolated microvessels will be of importance. Yet, despite caveats, freshly isolated microvessels provide an experimental preparation that has allowed us to make new observations and propose new hypotheses concerning the mechanisms by which angiotensin II regulates the retinal microvasculature.

In summary, by activating several types of ion channels, angiotensin II causes extracellular calcium to enter the pericytes of retinal microvessels. As a result, these cells contract, and microvascular lumens narrow. Adding

spatiotemporal complexity to these effects, angiotensin II also inhibits intercellular communication. Thus, this vasoactive signal not only regulates pericyte contractility, but also affects the functional organization of the retinal microvasculature.

References

- Barry PH (1994). JPCalc, a software package for calculating liquid junction potential corrections in patch-clamp, intracellular, epithelial and bilayer measurements and for correcting junction potential measurements. *J Neurosci Meth* **51**, 107–116.
- Fernandes R, Girao H & Pereira P (2004). High glucose down-regulates intercellular communication in retinal endothelial cells by enhancing degradation of connexin 43 by a proteasome-dependent mechanism. *J Biol Chem* **279**, 27219–27224.
- Grynkiwicz G, Poenie M & Tsien RY (1985). A new generation of Ca²⁺ indicators with greatly improved fluorescence properties. *J Biol Chem* **260**, 3440–3450.
- Herbert JM, Augereau JM, Gleye J & Maffrand JP (1990). Chelerythrine is a potent and specific inhibitor of protein kinase C. *Biochem Biophys Res Commun* **172**, 993–999.
- Kawamura H, Oku H, Li Q, Sakagami K & Puro DG (2002). Endothelin-induced changes in the physiology of retinal pericytes. *Invest Ophthalmol Vis Sci* **43**, 882–888.
- Kawamura H, Sugiyama T, Wu DM, Kobayashi M, Yamanishi S, Katsumura K & Puro DG (2003). ATP: a vasoactive signal in the pericyte-containing microvasculature of the rat retina. *J Physiol* **551**, 787–799.
- Kohler K, Wheeler-Schilling T, Jurklics B, Guenther E & Zrenner E (1997). Angiotensin II in the rabbit retina. *Vis Neurosci* **14**, 63–71.
- Kulkarni PS, Hamid H, Barati M & Butulija D (1999). Angiotensin II-induced constrictions are masked by bovine retinal vessels. *Invest Ophthalmol Vis Sci* **40**, 721–728.
- Kuwabara T & Cogan D (1960). Studies of retinal vascular patterns. 1: normal architecture. *Arch Ophthalmol* **64**, 904–911.
- Lampe PD, TenBroek EM, Burt JM, Kurata WE, Johnson RG & Lau AF (2000). Phosphorylation of connexin43 on serine368 by protein kinase C regulates gap junctional communication. *J Cell Biol* **149**, 1503–1512.
- Li Q & Puro DG (2001). Adenosine activates ATP-sensitive K⁺ currents in pericytes of rat retinal microvessels: role of A1 and A2a receptors. *Brain Res* **907**, 93–99.
- Li AF, Sato T, Haimovici R, Okamoto T & Roy S (2003). High glucose alters connexin 43 expression and gap junction intercellular communication activity in retinal pericytes. *Invest Ophthalmol Vis Sci* **44**, 5376–5382.
- Lindau M & Neher E (1988). Patch-clamp techniques for time-resolved capacitance measurements in single cells. *Pflugers Arch* **411**, 137–146.
- Mayer ML & Westbrook GL (1987). Permeation and block of N-methyl-D-aspartic acid receptor channels by divalent cations in mouse cultured central neurones. *J Physiol* **394**, 501–527.

- Moreno AP, Saez JC, Fishman GI & Spray DC (1994). Human connexin43 gap junction channels. Regulation of unitary conductances by phosphorylation. *Circ Res* **74**, 1050–1057.
- Moriarty P, Dickson AJ, Erichsen JT & Boulton M (2000). Protein kinase C isoenzyme expression in retinal cells. *Ophthalmic Res* **32**, 57–60.
- Nagahama T, Hayashi K, Ozawa Y, Takenaka T & Saruta T (2000). Role of protein kinase C in angiotensin II-induced constriction of renal microvessels. *Kidney Int* **57**, 215–223.
- Oku H, Kodama T, Sakagami K & Puro DG (2001). Diabetes-induced disruption of gap junction pathways within the retinal microvasculature. *Invest Ophthalmol Vis Sci* **42**, 1915–.
- Pallone TL & Huang JM (2002). Control of descending vasa recta pericyte membrane potential by angiotensin II. *Am J Physiol Renal Physiol* **282**, F1064–F1074.
- Rhinehart K, Zhang Z & Pallone TL (2002). Ca²⁺ signaling and membrane potential in descending vasa recta pericytes and endothelia. *Am J Physiol Renal Physiol* **283**, F852–F860.
- Sakagami K, Kawamura H, Wu DM & Puro DG (2001). Nitric oxide/cGMP-induced inhibition of calcium and chloride currents in retinal pericytes. *Microvasc Res* **62**, 196–203.
- Sakagami K, Wu DM & Puro DG (1999). Physiology of rat retinal pericytes: modulation of ion channel activity by serum-derived molecules. *J Physiol* **521**, 637–650.
- Schonfelder U, Hofer A, Paul M & Funk RH (1998). In situ observation of living pericytes in rat retinal capillaries. *Microvasc Res* **56**, 22–29.
- Shepro D & Morel NM (1993). Pericyte physiology. *FASEB J* **7**, 1031–1038.
- Suzuma I, Suzuma K, Ueki K, Hata Y, Feener EP, King GL & Aiello LP (2002). Stretch-induced retinal vascular endothelial growth factor expression is mediated by phosphatidylinositol 3-kinase and protein kinase C (PKC)-zeta but not by stretch-induced ERK1/2, Akt, Ras, or classical/novel PKC pathways. *J Biol Chem* **277**, 1047–1057.
- Tilton RG (1991). Capillary pericytes: perspectives and future trends. *J Electron Microscop Tech* **19**, 327–344.
- Wu DM, Kawamura H, Li Q & Puro DG (2001). Dopamine activates ATP-sensitive K⁺ currents in rat retinal pericytes. *Vis Neurosci* **18**, 935–940.
- Wu DM, Kawamura H, Sakagami K, Kobayashi M & Puro DG (2003). Cholinergic regulation of pericyte-containing retinal microvessels. *Am J Physiol Heart Circ Physiol* **284**, H2083–H2090.
- Zhang Z, Rhinehart K, Lee-Kwon W, Weinman E & Pallone T (2004). AngII signaling in vasa recta pericytes by PKC and reactive oxygen species. *Am J Physiol Heart Circ Physiol* **287**, H773–H781.
- Zhang Z, Rhinehart K & Pallone TL (2002). Membrane potential controls calcium entry into descending vasa recta pericytes. *Am J Physiol Regul Integr Comp Physiol* **283**, R949–R957.

Acknowledgements

The authors thank Bret Hughes for helpful discussions and use of equipment; Scott Salazay's technical expertise is greatly appreciated. This project was supported by a Physician-Scientist Training Award from the American Diabetes Association (D.M.W.), a Medical Student Research Fellowship (D.M.W.) and a Harrington Senior Investigator Award (D.G.P.) from Research to Prevent Blindness Inc., and grants EY12505 and EY07003 from the National Institutes of Health.

Supplementary material

The online version of this paper can be accessed at:

DOI: 10.1113/jphysiol.2004.073098

<http://jp.physoc.org/cgi/content/full/jphysiol.2004.073098/DC1> and contains the following supplementary material.

Time-lapse movie showing a freshly isolated rat retinal microvessel before, during and after addition of 500 nM angiotensin II to the perfusate

Differential interference contrast images were captured at 8 s intervals for a period of 16 min. The frames labelled 'angiotensin' indicate when this pericyte-containing microvessel was exposed to this vasoactive peptide. Two erythrocytes can be seen in the microvascular lumen. During exposure to angiotensin II, contraction of the pericyte located on the upper edge of the microvessel caused the adjacent lumen to narrow.

This material can also be found at:

<http://www.blackwellpublishing.com/products/journals/suppmat/tjp/tjp593/tjp593sm.htm>